Volume 21
Number 8
August 1982

Inorganic Chemistry

Contribution from the Department of Chemistry,
University of Wisconsin—Madison, Madison, Wisconsin 53706

Theoretical Study of *o*-Quinone Complexes of Chromium and Vanadium

DOUGLAS J. GORDON and RICHARD F. FENSKE*

Received July 6, 1981

Results of molecular orbital calculations on a number of *o*-quinone complexes of chromium and vanadium are presented. The unpaired electron in $[Cr(SQ)_2(bpy)]^+$ (SQ is *o*-semiquinone and bpy is 2,2′-bipyridine) is shown to occupy a metal-centered MO in accord with EPR results. A prediction is made about the electronic configuration of $[Cr(CAT)_2(bpy)]^-$ (CAT is catecholate), which has the same HOMO as the 1+ complex due to an inversion of the HOMO and LUMO in the 2-electron reduction. Calculations on $[Cr(SQ)_2(CAT)]^-$ indicate the unpaired electron occupies a metal-centered MO in agreement with the known EPR behavior of this complex. A 2-electron oxidation to form the $[Cr(SQ)_2(BQ)]^+$ (BQ is *o*-benzoquinone) complex leads to extremely small HOMO–LUMO separations but does not invert the order (relative to the 1− complex) as the EPR experiments suggest. The calculation on the $[V(SQ)_3]^{0+}$ complex, which is isoelectronic with the 1+ chromium complexes, correctly affirms that the unpaired electron is in a ligand-delocalized orbital. Calculations on tris(*o*-quinone)chromium complexes with overall charges of 0, 1−, 2−, and 3− correctly predict 0, 1, 2, and 3 unpaired electrons, respectively, and reproduce the features of the visible spectra of these complexes. Predictions of the electronic configuration of the 3+ and 2+ complexes are presented. The changes in metal–ligand bonding as the entire seven-membered series of tris(*o*-quinone)chromium complexes is traversed are discussed and are attributable to changes in the stability of the chromium 3d orbitals. Two different types of quinone ligands are predicted to be bound to chromium in the 2+, 1+, 1−, and 2− complexes. The charge on the chromium remains essentially constant over the seven-membered series. The added electron is distributed out to the ligands in agreement with an earlier explanation of these complexes.

Introduction

Transition-metal complexes of *o*-quinone ligands have received considerable attention in the past few years[1-5] and have been the subject of a recent review.[6] *o*-Benzoquinone is a terminal member of the redox series *o*-benzoquinone (**1**), *o*-benzosemiquinone (**2**), and catecholate (**3**). As might be

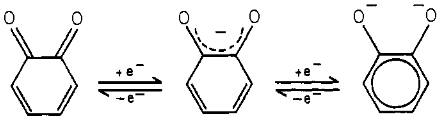

1 2 3

expected from this series, transition-metal complexes containing *o*-quinone ligands are rich in oxidation–reduction chemistry, exhibiting a wide range of oxidation states. Thus, the tris(3,5-di-*tert*-butyl-1,2-benzoquinone)chromium complexes exist with overall charges of 2+ through 3− in unit steps.[2-4] Because *o*-quinones are "noninnocent ligands", defining the oxidation state of the metal and ligands in these complexes can be difficult.

Oxidation states for ligands and metal in these compounds have usually been assigned on the basis of the carbon–oxygen, carbon–carbon, and metal–oxygen bond lengths by a comparison to other complexes with similar metal oxidation states and with the free-ligand interatomic distances. Pierpont and co-workers[4] have proposed a model for the seven-membered tris(9,10-phenanthrenequinone)chromium redox series in which the neutral complex is considered to be a high-spin chromium(III) antiferomagnetically coupled to three semiquinone ligands. Stepwise reduction or oxidation of the neutral complex is postulated to leave the charge on the chromium unchanged with the electron added to or removed from a ligand, decoupling a metal electron. Qualitative molecular orbital arguments by Raymond and co-workers[2,3] using a bonding model involving one filled σ (oxygen lone pair) orbital and one empty π^* (oxygen–carbon antibonding) orbital per oxygen to give a CrO_6 chromophore of T_h symmetry predict the LUMO in chromium tris(3,5-di-*tert*-butyl-*o*-quinone) is a π-antibonding level. More detailed predictions are not possible in view of the fact that no quantitative theoretical investigation of these complexes has been done.

We have successfully treated relatively large transition-metal complexes such as $CH_3Mn(CO)_5$,[7] $Mn(CO)_{5-n}(CNCH_3)_nBr$ for n = 0, 1, 2, 3, and 4,[8] and $CpFe(CO)_2X$ for X = Cl, Br, I, and CH_3[9] by a nonempirical approximate molecular orbital method known as the Fenske–Hall method. It is the purpose of this paper to present the results of our calculations on $[M(L)_2(L')]^n$ for (1) M = Cr, L = L′ = *o*-quinone, and n ranging from 3+ to 3−, (2) M = V, L = L′ = *o*-quinone, and n = 0, and (3) M = Cr, L = *o*-quinone, L′ = 2,2′-bipyridine, and n ranging from 1+ to 1−. The effects on the electronic structure and bonding properties of these complexes as well

---

(1) Raymond, K. N.; Isied, S. S.; Brown, L. D.; Fronczek, F. R.; Nibert, J. H. *J. Am. Chem. Soc.* **1976**, *98*, 1767–1774.
(2) Sofen, S. R. Ph.D. Thesis, University of California, Berkeley, CA, 1979.
(3) Sofen, S. R.; Ware, D. C.; Cooper, S. R.; Raymond, K. N. *Inorg. Chem.* **1979**, *18*, 234–239.
(4) Downs, H. H.; Buchanan, R. M.; Pierpont, C. G. *Inorg. Chem.* **1979**, *18*, 1736–1740.
(5) Buchanan, R. M.; Pierpont, C. G.; *J. Am. Chem. Soc.* **1980**, *102*, 4951–4957.
(6) Pierpont, C. G.; Buchanan, R. M. *Coord. Chem. Rev.* **1981**, *38*, 45–87.
(7) Hall, M. B.; Fenske, R. F. *Inorg. Chem.* **1972**, *11*, 768–775.
(8) Sarapu, A. C.; Fenske, R. F. *Inorg. Chem.* **1975**, *14*, 247–253.
(9) Lichtenberger, D. L.; Fenske, R. F. *J. Am. Chem. Soc.* **1976**, *98*, 50–63.

0020-1669/82/1321-2907$01.25/0

as the overall charge changes are presented. The shift in the frontier molecular orbitals on substitution of vanadium for chromium is explored and is related to the observed differences in the electron paramagnetic resonance (EPR) spectra of isoelectronic complexes. The effects of substituting alkyl groups (including methyl and *tert*-butyl) at the 3- and 5-positions on the benzene ring are described. The effects on the electronic structure of the chromium complexes as an *o*-quinone ligand is replaced by a bipyridine ligand are considered. The preferred description of metal and ligand oxidation states is discussed. The distribution of charge when the oxidized members of the series are reduced is outlined. Correlations are presented with existing structural, magnetic susceptibility, and spectral (both UV–visible and EPR) data, and predictions are made about those complexes that have not been so completely studied.

Method

The calculational method used, Fenske–Hall, is a nonempirical molecular orbital method and has been described previously.[6] Because the method uses no adjustable parameters, the final results depend only upon the choice of atomic basis functions and molecular geometry.

Clementi's double-ζ functions for neutral atoms were used for carbon, nitrogen, and oxygen.[10] The 1s and 2s functions were curve-fit to single ζ by using the maximum overlap criterion, while their orthogonality was maintained.[11] An exponent of 1.16, which corresponds to the minimum-energy exponent for methane,[12] was used for hydrogen. Metal functions were taken from the results of Richardson et al.[13] and were chosen to correspond to M(II) on the basis of charge considerations. All metal basis functions were single ζ except the 3d, which were double ζ.

Molecular geometries were derived from published crystal structures when available. Thus, the catecholate (CAT) coordinates were obtained from the structure of $K_3[Cr(CAT)_3]$ by Raymond et al.[1] The semiquinone (SQ) coordinates were derived from the structure of tris(3,5-di-*tert*-butyl-1,2-benzoquinone)chromium[3] ($[Cr(3,5\text{-}DBSQ)_3]^{0+}$), by replacement of the *tert*-butyl groups by hydrogens. The benzoquinone (BQ) positional parameters were derived by analogy to the only known benzoquinone crystal structure, namely, dichlorodioxo(9,10-phenanthrenebenzoquinone)molybdenum[14] from which the Cr–O distances were obtained by covalent radii considerations. The intraligand bond distances and angles were taken to be the same as in the free BQ ligand.[15] The 2,2′-bipyridine (bpy) geometry was taken from the analogous cobalt complex bis(3,5-di-*tert*-butyl-1,2-benzoquinone)(2,2′-bipyridine)cobalt[5] with the Cr–N bond distance determined by the difference between the covalent radii of cobalt and chromium. The six oxygen atoms in the tris(*o*-quinone) complexes are coordinated to the central metal in an octahedral fashion with the six carbons of the ring and their substituents all coplanar, giving the coordination sphere D_3 symmetry. Replacement of one of the *o*-quinone ligands by bipyridine lowers the symmetry to C_2. The 3,5-dimethyl and 3,5-di-*tert*-butyl coordinates were derived from the corresponding unsubstituted ligands by simple replacement of the appropriate hydrogen by the alkyl group.

EPR Results

The electron paramagnetic resonance spectra of a number of *o*-quinone complexes of vanadium and chromium have been determined previously. To facilitate the discussion of our results, it is useful to first summarize the EPR results.

The unpaired electron in tris(3,4,5,6-tetrachlorobenzoquinone)vanadium exhibits a ^{51}V hyperfine coupling constant of only 4.1 G.[16] The small value for the ^{51}V hyperfine coupling constant for this complex is typical of semiquinone complexes with the unpaired electron spin density localized on the ligand. The ^{51}V hyperfine coupling constant is small for the tris(3,5-di-*tert*-butyl-1,2-benzoquinone)vanadium complex,[17] although a complete interpretation of the spectrum is complicated by coupling to the *tert*-butyl protons at the 5-position and the ring proton at the 4-position.

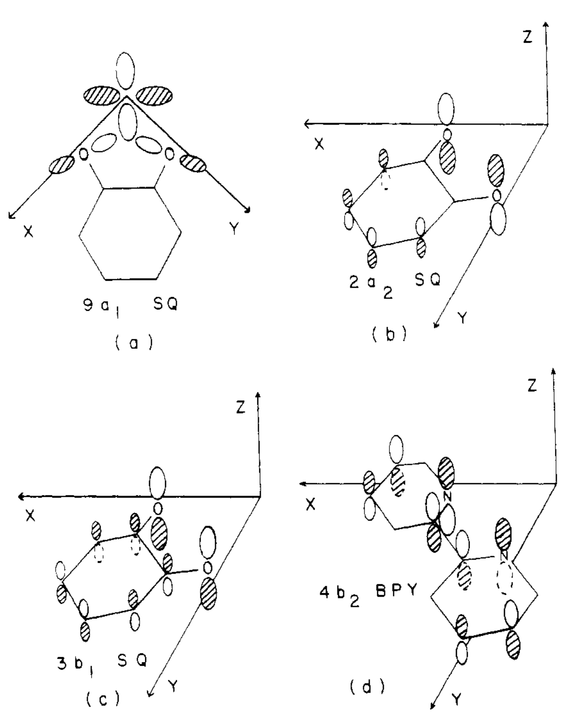

Figure 1. Representations for the *o*-semiquinone (SQ) and 2,2′-bipyridine (bpy) basis orbitals that contribute to the valence MOs of the complexes considered here. All ligands shown lie in the *XY* plane. Shaded regions represent areas where the sign of the wave function is negative.

In contrast to the neutral vanadium complexes, the isoelectronic CrL_3^+ (L = 3,4,5,6-tetrachlorobenzoquinone, 3,5-di-*tert*-butyl-1,2-benzoquinone, or 9,10-phenanthrenequinone) complexes show the strongest metal hyperfine coupling yet observed for *o*-quinone transition-metal complexes. The ^{53}Cr hyperfine coupling constants for the 1+ complexes are in the range of 27–28 G[4] and are very similar to the ^{53}Cr hyperfine coupling constants for the analogous 1– complexes. Furthermore, the *g* values for the corresponding 1+ and 1– complexes are very similar and show an orbital contribution. These results may be explained from a molecular orbital point of view by assuming the odd electron is in a molecular orbital with a large metal character. The similarity in hyperfine coupling constants and *g* values for corresponding 1– and 1+ complexes may be explained by assuming the odd electron is in the same metal-centered molecular orbital; the addition of 2 electrons causes the LUMO of the 1+ complex to be lower in energy than the HOMO, resulting in the singly occupied level being the same MO for the 1+ and 1– complexes. The above explanation has been previously advanced[4] by analogy with molecular orbital calculations on the isoelectronic tris(diimine) complexes of chromium.[18]

The isoelectronic bipyridine system formed by replacement of the benzoquinone ligand in $Cr(SQ)_2(BQ)^+$ by bpy shows ^{53}Cr hyperfine coupling constants that range from 25 to 26 G.[17,19] The ^{53}Cr hyperfine coupling constants as well as the

---

(10) Clementi, E. *J. Chem. Phys.* **1964**, *40*, 1944–1945.
(11) Radtke, D. D. Ph.D. Thesis, University of Wisconsin, Madison, WI, 1966.
(12) Hehre, W. J.; Stewart, R. F.; Pople, J. A. *J. Chem. Phys.* **1969**, *51*, 2657–2664.
(13) Richardson, J. W.; Nieupoort, W. C.; Powell, R. R.; Edgell, W. F. *J. Chem. Phys.* **1962**, *36*, 1057–1061.
(14) Pierpont, C. G.; Downs, H. H. *Inorg. Chem.* **1977**, *16*, 2970–2972.
(15) Macdonald, A. L.; Trotter, J. J. *J. Chem. Soc., Perkin Trans. 2* **1973**, 476–480.
(16) Buchanan, R. M.; Downs, H. H.; Shorthill, W. B.; Pierpont, C. G.; Kessel, S. L.; Hendrickson, D. N. *J. Am. Chem. Soc.* **1978**, *100*, 4318–4320.
(17) Pierpont, C. G., private communication.
(18) Hanayaki, I.; Nagakura, S. *Bull. Chem. Soc. Jpn.* **1971**, *44*, 2312–2321.

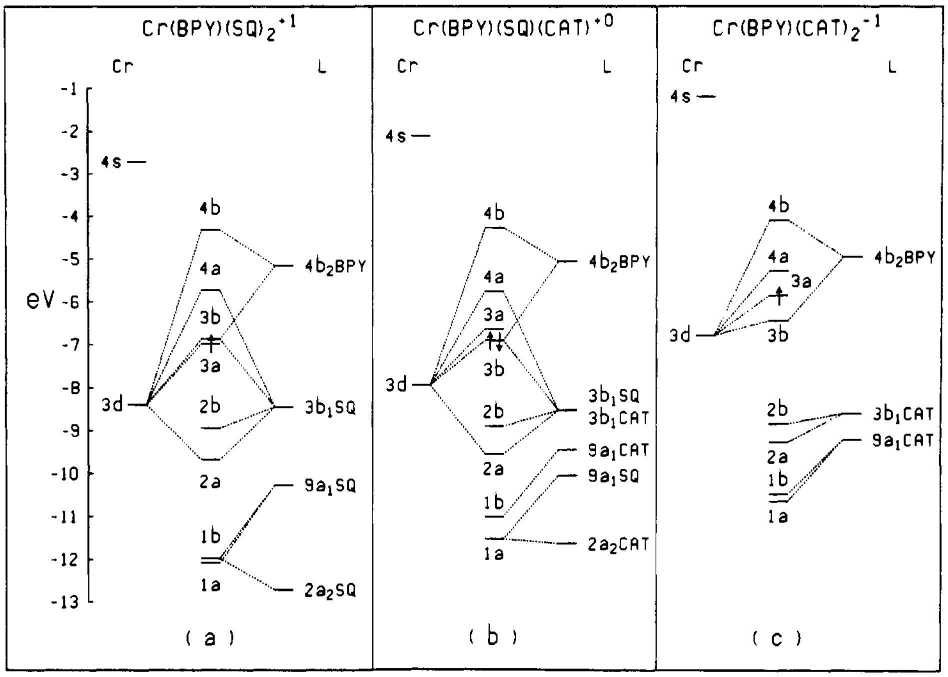

Figure 2. Molecular orbital diagrams for bis(*o*-quinone)(bipyridine)chromium complexes. HOMO is indicated by an arrow or arrows representing an electron. See text for an explanation of ligand names.

g values are extremely similar for $Cr(SQ)_2(bpy)^+$ and $Cr(SQ)_2(BQ)^+$ for the three *o*-quinone ligands mentioned above. Thus, we would again expect that the odd electron in the $Cr(SQ)_2(bpy)^+$ system is in a molecular orbital which is strongly metal in character.

A proper theoretical interpretation of the electronic structure of these systems should be in accord with the EPR data, particularly with respect to the substantial differences in the behavior between the vanadium and chromium complexes.

Results and Discussion

Free Ligands. Figure 1 shows how the *o*-quinone and bipyridine ligands in the *XY* plane interact with the central metal. Representations are given for all ligand basis orbitals that contribute significantly to the valence molecular orbitals of the complexes considered. The positions of the oxygen and nitrogen atoms are indicated by O and N, respectively, with all other vertices assumed to be occupied by carbon atoms. The hydrogen atoms have been omitted for the sake of clarity. The symmetry labels are taken from the C_{2v} point group while SQ represents *o*-semiquinone (the results are virtually identical for either free *o*-benzoquinone or free catecholate) and bpy represents 2,2′-bipyridine. Shaded regions represent areas where the sign of the wave function is negative whereas the wave function is positive in unshaded regions. Orbital lobes outlined with broken rather than solid lines lie below the rings shown and out of the observer's direct line of sight.

Figure 1a shows the $9a_1$ orbital for *o*-semiquinone, which interacts with the d_{xy} orbital of the metal in a σ fashion. The $9a_1$ orbital is localized on the ortho oxygens and is the highest occupied molecular orbital (HOMO) in the neutral *o*-benzoquinone representing an oxygen lone pair. The $2a_2$ and $3b_1$ *o*-semiquinone orbitals, presented in Figure 1b,c, interact with the metal d orbitals in a π fashion. The oxygen lying near the *X* axis interacts with the d_{xz} orbital while the oxygen lying near the *Y* axis interacts with the d_{yz} orbital. Both orbitals are primarily localized on the oxygen atoms with a significant amount of delocalization over the rest of the ring. The $2a_2$ orbital is a carbon–oxygen π-bonding level, which is doubly occupied in the free *o*-semiquinone. The $3b_1$ orbital in the *o*-quinone is a carbon–oxygen π^*-antibonding orbital. In the neutral *o*-benzoquinone the $3b_1$ level is the lowest unoccupied molecular orbital (LUMO). Thus the $3b_1$ orbital contains 0, 1, and 2 electrons for free *o*-benzoquinone, *o*-semiquinone, and catecholate, respectively. The $4b_2$ orbital on the 2,2′-bipyridine shown in Figure 1d interacts with the metal d orbitals in a manner analogous to that for $2a_2$ and $3b_1$ of the *o*-semiquinone. The $4b_2$ orbital is a ring π^*-antibonding level whose largest contribution is from the $p\pi$ orbital on the nitrogens but is considerably more diffuse than either the $2a_2$ or the $3b_1$ SQ orbitals. The $4b_2$ orbital is the LUMO in free bipyridine with a very large separation in energy between the HOMO and LUMO when compared to the case of the *o*-quinones. Because they make the largest ligand contribution to the valence molecular orbitals of the complexes considered, here we will be primarily interested in how the $3b_1$ *o*-quinone and $4b_2$ bipyridine basis orbitals interact with the d orbitals on the metal.

$Cr(Q)_2(bpy)^n$ (n = 1+, 0, 1−) (Q = *o*-Quinone). Figure 2 presents a comparison of the results of our calculations on the bis(*o*-quinone)(bipyridine)chromium complexes with overall charges of 1+, 0, and 1−. A common energy scale in electronvolts appears on the left side of the figure. In this and all subsequent figures comparing calculations on complexes with different overall charges an approximately constant value of 3.8 eV/unit charge has been added to or subtracted from all energies obtained directly from the calculations to reflect the presence of counterions. The three molecular orbital diagrams are presented with the energies of the chromium basis orbitals in the left-hand column, those of the ligand basis functions in the right column, and the eigenvalues of the molecular orbitals in the central column. All occupied levels starting with the metal–*o*-quinone σ-bonding orbitals are shown as well as the lowest few unoccupied molecular orbitals. The highest occupied molecular orbital is indicated by an arrow (or arrows) representing an electron (or electrons). All molecular orbitals below the HOMO are doubly occupied. The symmetry labels for the molecular orbitals are taken from the C_2 point group symmetry of the 1+ and 1− complexes with the neutral complex being assigned by analogy.

As shown in Figure 2, the 4s orbital is much higher in energy than the 3d orbitals. The 4p orbitals (not shown) are even

---

(19) Buchanan, R. M. Ph.D. Thesis, University of Colorado, Boulder, CO, 1980.

higher in energy. Because of symmetry considerations and the large separation between the energies of the 4s and 4p orbitals on the metal and ligand basis orbitals, there is very little interaction between them. The 4s levels will be omitted in future figures for simplicity.

The labels for the ligand orbitals require some explanation. Where an SQ is attached, it means that the basis orbital comes from a ligand whose metal–oxygen, carbon–oxygen, and carbon–carbon bond distances correspond to a semiquinone type ligand, while a CAT label means that basis orbital is from a catecholate type ligand. If a bpy is appended, it means that the basis orbital comes from a 2,2′-bipyridine ligand. The crystal structures of these complexes have not been published. We performed calculations on the 1+ complex in two different geometries, one in which the bpy ligand replaced the BQ ligand of the analogous $Cr(SQ)_2(BQ)^+$ complex and the other in which bpy replaced an SQ ligand. There is a clear energetic preference[20] for the $Cr(bpy)(SQ)_2^+$ geometry used in Figure 2a. Since we are primarily interested in the character of the HOMO, which was mainly metal for either geometry, we present the results for the lowest energy geometry only.

The $9a_1$ level on the *o*-quinone ligands is stabilized by a bonding interaction with the metal to form the 1a and 1b molecular orbitals. The bpy σ-bonding levels are much lower in energy, and since their inclusion adds nothing to the present discussion, they have been omitted for compactness. The $3b_1$ orbital on the *o*-quinone ligands interacts with the metal to form a bonding and a nonbonding molecular orbital, the 2a and 2b MOs, respectively. As shown in Figure 2a, the HOMO for $Cr(bpy)(SQ)_2^+$ is the singly occupied 3a orbital, which is strongly localized on the metal, having 80% metal, 2% bpy, and 9% each SQ character. In contrast, the 3b LUMO is delocalized over the whole complex and comprises 37% metal, 27% bpy, and 17% each SQ character. The extremely small separation between the 3a HOMO and the 3b LUMO of only 0.2 eV is outside of our previous experience with the Fenske–Hall method. The 4a and 4b molecular orbitals are antibonding orbitals formed by interaction of the metal d orbitals with the $3b_1$ SQ and $4b_2$ bpy orbitals, respectively.

Interestingly, when the 1+ complex is reduced to the neutral $Cr(bpy)(SQ)(CAT)^{0+}$ complex, a reversal of the HOMO and LUMO occurs as shown in the diagram in Figure 2b. Now the HOMO is the delocalized 3b molecular orbital, which is doubly occupied, and the LUMO is the metal-localized 3a MO. A comparison of parts a and b of Figure 2 shows the reason for this inversion. With addition of an electron the energies of the $3b_1$ orbital on the *o*-quinone ligands and the $4b_2$ orbital on bipyridine remains essentially constant while the 3d level on chromium is destabilized. Because the 3b MO has a smaller metal character, it is less stabilized than the strongly metal 3a, and coupled with the small 3a–3b separation in Figure 2a, the order inverts. Adding another electron to the neutral complex yields the $Cr(bpy)(CAT)_2^-$ complex and may be seen from Figure 2c leads to a further destabilization of the 3d orbitals on chromium. The added electron populates the metal-localized 3a MO, which has increased its separation from the delocalized 3b MO. The 3a MO is less stabilized than the 3d orbitals because of the decreasing interaction between the 3d orbitals and the lower energy *o*-quinone basis orbitals.

Thus, Figure 2 presents the results of our calculations on the bis(*o*-quinone)(bipyridine)chromium complexes in which the addition of 2 electrons to the paramagnetic 1+ complex with a metal-localized HOMO causes an inversion of the HOMO and LUMO, resulting in the HOMO of the 1− complex having the same basic character as the HOMO of the 1+ complex. The large chromium contribution to the HOMO of the $Cr(bpy)(SQ)_2^+$ complex is in excellent agreement with the EPR results discussed earlier (see the Appendix for a discussion of the transferability of results on unsubstituted *o*-quinone calculations to substituted *o*-quinone calculations).

We are unaware of any EPR or magnetic susceptibility results on the $Cr(bpy)(CAT)_2^-$ complex. In Pierpont's formulation of this complex[17] the high-spin Cr(III) should be paramagnetic by 3 electrons. It can be seen in Figure 2c that our calculations show a relatively small separation between the doubly occupied 3b MO and the 4a LUMO. Because the 3a and 4a MOs are localized on the metal while the 3b MO is delocalized substantially on the bpy ligand, we prefer a low-spin description of this complex. Further work needs to be done on this complex in order to clarify the total spin of the ground state.

$Cr(Q)_3^n$ (n = 1+, 0, 1−). Figure 3 presents a comparison of the molecular orbital diagrams for the tris(*o*-quinone)-chromium complexes of overall charges 1+, 0, and 1− obtained from our results. The labels for the ligand basis functions are analogous to those in Figure 2. The crystal structures of the 1+ and 1− complexes are unknown. We performed calculations on the 1+ complex in two different geometries, one in which all three ligands were the same, of SQ type, and the second as indicated in Figure 3a. There was a clear energetic preference[20] for the symmetry-lowered geometry of Figure 3a. The symmetry labels for the molecular orbitals are taken from the D_3 point group despite the C_2 symmetry of the 1+ and 1− complexes for ease of comparison. Where the degenerate e levels are split due to the lower symmetry, a (1) or (2) is attached to the label to identify the two components. All molecular orbitals lower in energy than the HOMO are fully occupied.

Examination of Figure 3c reveals that the unpaired electron is in the a_1 MO, which is localized on the chromium. This result compares favorably with the molecular orbital explanation of the large ^{53}Cr hyperfine coupling constant of the 1− chromium complexes presented earlier. Upon removal of an electron to go to the neutral complex, the energy separation between the a_1 LUMO and the a_2 HOMO (which is delocalized over the three semiquinone ligands) has decreased as shown by a comparison of Figure 3b which Figure 3c. The reason for this decreasing energy difference is that the large stabilization of the 3d orbitals on the chromium is partially offset by a smaller stabilization of the $3b_1$ orbitals on SQ. Oxidation of the neutral complex to give the 1+ complex leads to a further decrease in the energy of separation of the HOMO and LUMO. These extremely small HOMO–LUMO separations (~0.2 eV in this case) are new to us. In this case the HOMO is predicted to be the a_2 MO delocalized over the *o*-quinone ligands with no metal contribution. This result is at odds with the EPR results discussed previously, which would most readily be explained by an inversion of the order of the a_2 and a_1 MOs. The decrease in the energy of separation of the a_1 and a_2 MOs is due to the smaller destabilization of the 3d orbitals on chromium and destabilization of the $3b_1$ orbital on BQ (as compared to SQ), which mitigates the stabilization of the $3b_1$ orbital on the SQ ligands.

The failure to invert the order of the a_2 and a_1 MOs in the $Cr(SQ)_2(BQ)^+$ calculation is not due to our choice of basis sets. A variety of calculations were performed on the 1+ complex by using more diffuse and more localized functions in various combinations on the chromium atom and oxygen atoms to reflect differing electronegativities and degrees of covalency in the metal–oxygen bonds. The order of the a_2 and a_1 MOs remained the same in all cases considered. The ob-

---

(20) Based on a total energy obtained by a sum of 1-electron eigenvalues of those occupied molecular orbitals most strongly affected by the geometry change considered. In doing this, we assumed all other occupied levels to be unaffected and their energies to remain constant.

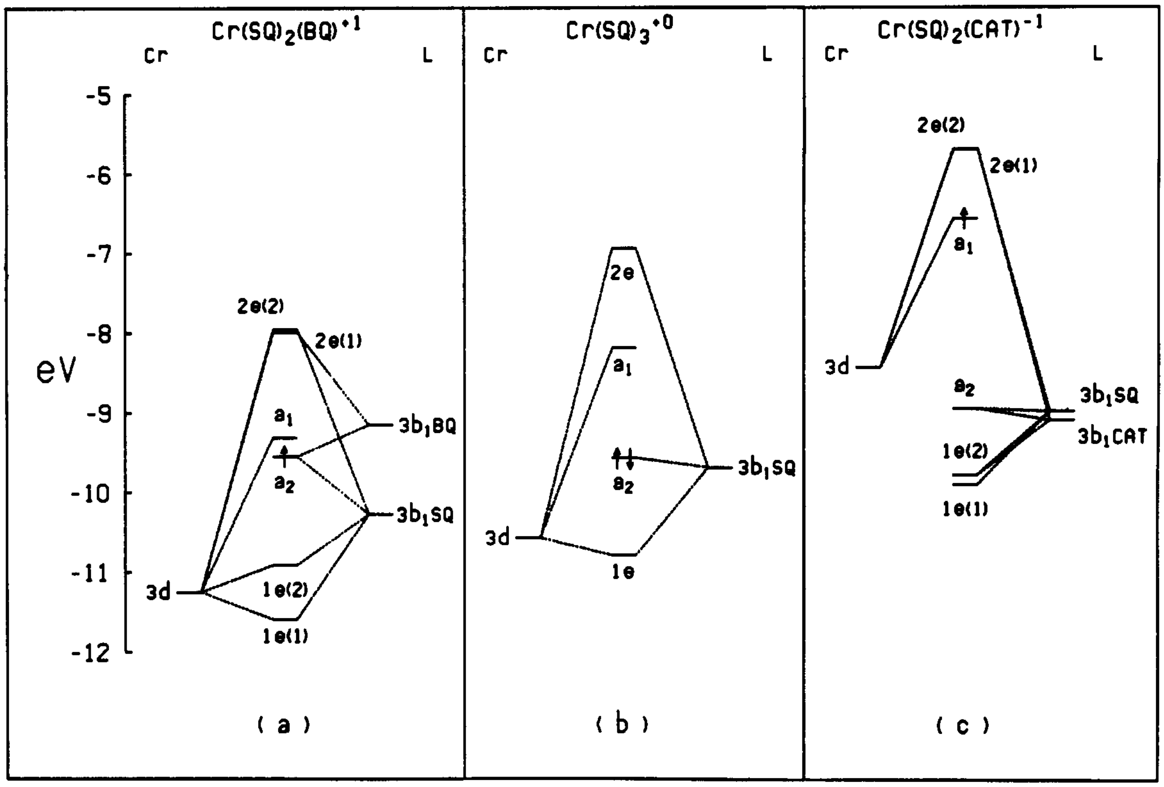

Figure 3. Molecular orbital diagrams for $[Cr(Q)_3]^n$ (n = 1−, 0, 1+). HOMO is indicated by an arrow or arrows representing an electron. See text for an explanation of ligand abbreviations.

served ^{53}Cr hyperfine coupling for the 1+ complex may not be explained by assuming a thermal population of the a_1 MO from the a_2 MO. Pierpont and co-workers[18] have performed temperature-dependent EPR experiments on the chromium 1+ complexes down to liquid nitrogen temperature. Contrary to what would be expected if a thermal population mechanism were operative, as the temperature is lowered, signals due to ^{53}Cr hyperfine interaction sharpen until the solvent solidifies, after which the ^{53}Cr hyperfine interaction is lost. There is, however, no change in the g value for the complex down to 77 K.

The the order of the a_2 and a_1 MOs is not inverted in the 1+ calculation when compared to the 1− calculation as they should be is due to the approximate nature of the Fenske–Hall method. For example small changes in the off-diagonal elements of the approximate Fock matrix could bring about the desired inversion. Furthermore the open-shell nature of the problem might be a contributing factor as the Fenske–Hall method was developed with the assumption of a closed-shell system. Rather than make any "minor adjustment" in the calculational approach that would yield the desired energy level sequence, we prefer to accept the shortcomings of the computational method and recall that the results of approximate molecular orbital calculations must be interpreted with care especially when one is dealing with open-shell systems having extremely small separations between important MOs such as in Figure 3a.

$V(Q)_3^{0+}$. The results of our calculations on the tris(*o*-quinone)vanadium neutral complex are presented in the molecular orbital diagram shown in Figure 4. The energy scale and symmetry labels are as described previously. The crystal structure of this complex has not been completely solved owing to instability, but the tris(tetrachloro-1,2-benzoquinone) complex of V has been shown to be isostructural with the tris(tetrachloro-1,2-benzoquinone) complexes of Cr and Fe,[16] which contain three equivalent semiquinone ligands. Results of EPR experiments considering ^1H hyperfine interactions with the *tert*-butyl protons and the ring proton at the 4-position of tris(3,5-di-*tert*-butyl-1,2-benzoquinone)vanadium indicate at least two equivalent quinone ligands. We have performed calculations on the tris(*o*-quinone)vanadium neutral complex in two geometries: one with two ligands of SQ type and the third of BQ type and another geometry as shown in Figure 4. There is no clear energetic preference for one geometry over another. However, since we are mainly interested in the character of the HOMO and LUMO (which are almost exactly the same in either geometry), we present results for the D_3 symmetry geometry consistent with the partial structural determination.

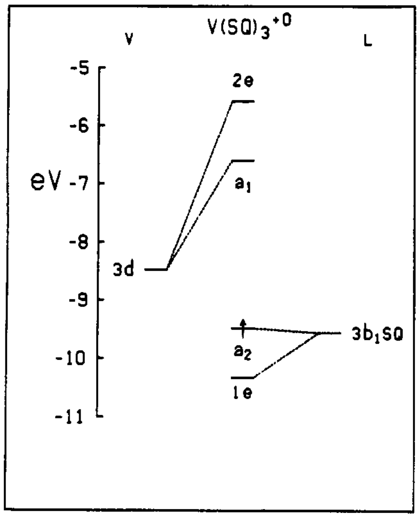

Figure 4. Molecular orbital diagram for the tris(*o*-quinone)vanadium complex. HOMO is indicated by an arrow representing an electron. SQ represents a semiquinone type ligand.

As Figure 4 shows, the unpaired electron resides in the a_2 MO, which is delocalized over the three SQ ligands and is well separated (~3 eV) from the metal-localized a_1 LUMO. The odd electron occupying a ligand-delocalized MO is again en-

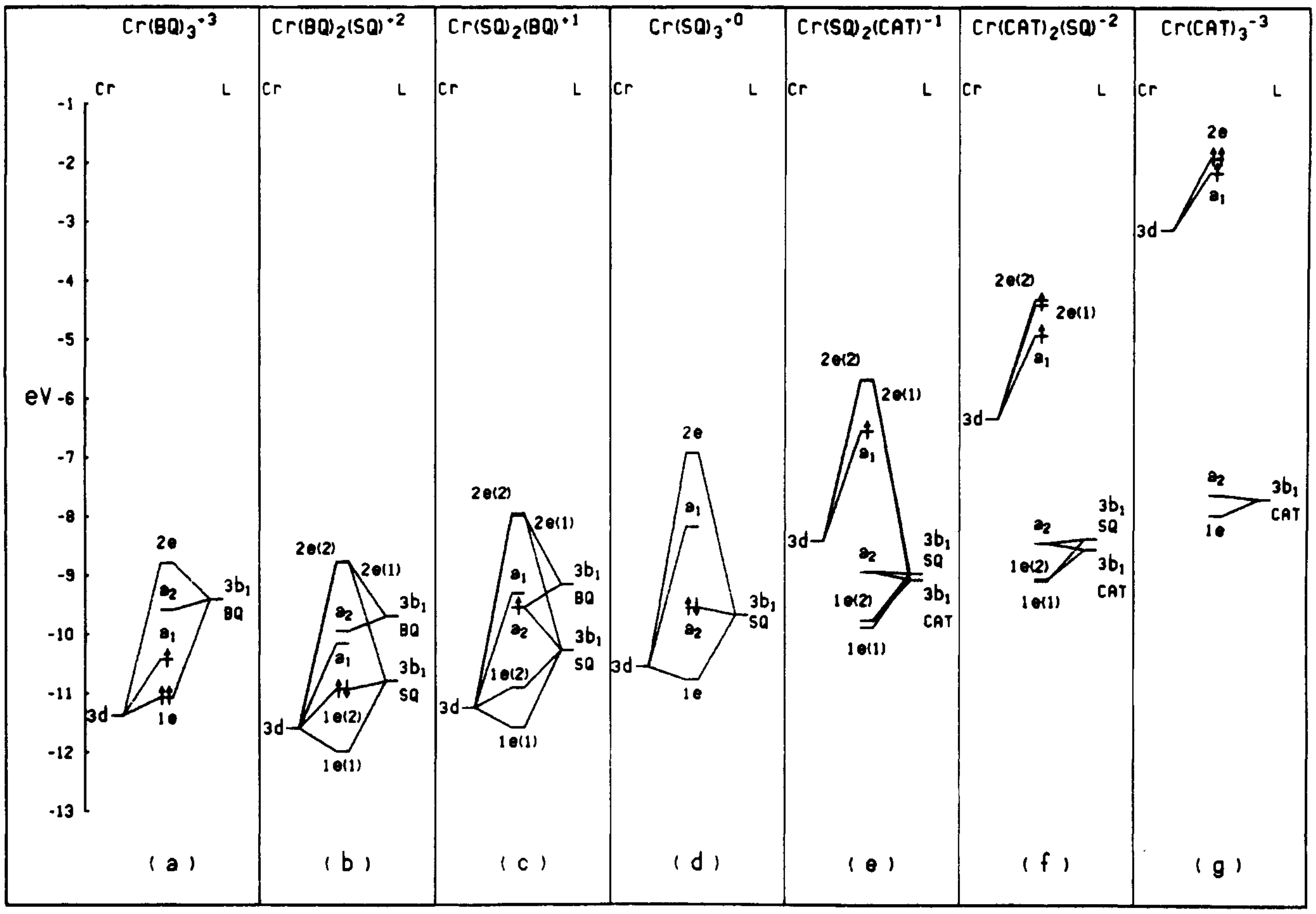

Figure 5. Molecular orbital diagrams for the seven-membered redox series of tris(*o*-quinone)chromium complexes. The occupation of the highest (few) occupied molecular orbital(s) is indicated by an arrow or arrows representing an electron. Arrows with the same direction represent electrons having the same spin. All levels below those containing arrows are completely filled. See text for an explanation of the ligand abbreviations.

tirely consistent with the observed small ^{51}V hyperfine interaction described previously. The HOMO–LUMO separation for the V neutral complex is much larger than for the isoelectronic Cr 1+ complex. Comparison of Figure 4 with Figure 3a reveals the reason for this difference. The 3d orbitals of V are much less stable (relative to the $3b_1$ orbital of the *o*-quinones) than the 3d orbitals on Cr. This fact, coupled with the essentially nonbonding character of the a_2 MO, leads to the large HOMO–LUMO separation for the V complex and the small separation in the Cr 1+ case and may easily be used to rationalize the qualitatively different behavior of the isoelectronic V neutral and Cr 1+ complexes. Thus, it appears that the additional stability of the 3d orbitals on Cr due to the presence of one more proton in the nucleus causes the inversion in the order of the a_2 and a_1 MOs on going from V to Cr for the isoelectronic complexes discussed here.

$Cr(Q)_3^n$ (n = 3+, ..., 3–). Figure 5 presents the results of our calculations on the seven-membered redox series of tris(*o*-quinone)chromium complexes with overall charges ranging from 3+ to 3–. The symmetry labels used are as in Figure 4. The ligand type for the $3b_1$ orbital appears below that label with BQ, SQ, and CAT having the same meaning as earlier. A discussion of our results on this seven-membered series may be conveniently divided into two parts. The first part consists of three anionic complexes and the neutral complex for which a number of experimental data exist, while the second part consists of three cationic complexes that are less well characterized.

As mentioned earlier, the neutral tris(*o*-quinone)chromium complex has a doubly occupied HOMO, the a_2 MO. Upon reduction of the neutral complex to form the 1– complex, the 3d orbitals are destabilized relative to the $3b_1$ orbitals of the ligands and the unpaired electron occupies the metal-centered a_1 MO. Reducing the 1– complex to the 2– complex causes a further destabilization of the 3d orbitals as compared to the $3b_1$ orbitals of the *o*-quinones. As may be seen in Figure 5f, the separation between the a_1 and 2e MOs decreases. The bonding is becoming more ionic, with the 1e and a_2 MOs delocalized over the ligands and the a_1 and 2e MOs localized on Cr and with very little interaction between metal and ligands. Because of the relatively small separation in energy and the metal-localized nature of the a_1 and 2e MOs, we performed a simple crystal field type calculation[21] in order to get an idea of the difference in energy between the singlet and triplet states. This calculation yields a $^1A_1$–^3E energy difference of 2.5 eV, which is over 4 times the separation between the a_1 and 2e MOs. Even with allowance for the simplicity of the model, these numbers indicate the spin-pairing energy should be larger than the energy required to promote an electron from the a_1 MO to the 2e MO and lead us to predict a triplet ground

---

(21) Consideration of the appropriate Coulomb and exchange integrals yields the following expression for the difference in energy between the singlet and triplet states in the d^2 case:

$$\Delta E(\text{singlet–triplet}) = 12F_2 + 45F_4$$

The corresponding expression for the energy difference in the d^3 case is

$$\Delta E(\text{doublet–quartet}) = 4F_2 + 120F_4$$

by using the symbolism and Coulomb and exchange integrals from: Ballhausen, C. J. "Introduction to Ligand Field Theory"; McGraw-Hill: New York, 1962; p 76. Values used for the F_2 and F_4 integrals correspond to Cr(II) in order to reflect the charge on chromium in the complex environment.

state for the 2− complex. Reducing the 2− complex to the 3− complex again leads to a large destabilization of the 3d orbitals on chromium. The a_1–2e separation decreases as shown in Figure 5g. Crystal field calculations of the type mentioned earlier[21] yield a ^2E–$^4A_2$ energy difference of 2.0 eV, which is 8 times the a_1 2e energy difference. Applying reasoning analogous to that above leads us to predict the 3− complex has a quartet ground state. Raymond and co-workers[2,3] have performed solution magnetic susceptibility experiments on tris(3,5-di-*tert*-butyl-1,2-benzoquinone)chromium complexes with overall charges of 0, 1−, 2−, and 3−. They interpret the results of their studies to mean there are 0, 1, 2, and 3 unpaired electrons in the neutral, 1−, 2−, and 3− complexes, in excellent agreement with our results.

Our results on the anionic series of complexes are also in good qualitative agreement with the visible spectra reported for these complexes.[2,3] Examination of Figure 5d leads one to expect a rich spectrum as all transitions from occupied to virtual MOs are symmetry and orbitally allowed. Furthermore, because these transitions (e.g., $a_2 \rightarrow a_1$, $a_2 \rightarrow 2e$, $1e \rightarrow a_1$, and $1e \rightarrow 2e$) are of a ligand to metal charge-transfer type, we would expect to see visible absorption bands with large extinction coefficients. Adding electrons to reduce the neutral complex leads to an increasing separation between the ligand-centered 1e and a_2 MOs and the metal-centered a_1 and 2e MOs as shown in Figure 5e–g. Finally, in the 3− complex the only low-energy transitions are of d → d type, which we would expect to give rise to a spectrum with no bands in the visible region having large extinction coefficients. The visible absorption spectra of the tris(3,5-di-*tert*-butyl-1,2-benzoquinone)chromium complexes with charges of 0, 1−, 2−, and 3− as obtained by Raymond and co-workers exhibit these features.

Turning now to the cationic series, we recall the results of our calculations on the 1+ complex show a very small HOMO–LUMO separation with the calculated order at odds with the EPR data, which we postulated was due to small errors in the approximate Fock matrix. Removing an electron from the 1+ complex gives the 2+ complex, whose molecular orbital diagram is shown in Figure 5b. As can be seen from the figure, there is an approximately uniform stabilization of all basis orbitals upon removing the electron from the 1+ complex. Changes in the character of the a_2 MO have resulted in the order of the a_1 and a_2 MOs being inverted. The HOMO is the 1e(2) MO, which is a metal–ligand bonding orbital with approximately equal proportions of 3d and $3b_1$ character.

We have indicated the ground state of the molecule to be a singlet although because of the proximity of the HOMO and LUMO we cannot rule out the possibility that it is a triplet. We prefer the singlet-state interpretation for several reasons. The 1e(2) MO is delocalized over the metal and ligands while the a_1 MO is localized on the metal; hence, promotion of an electron from the 1e(2) MO to the a_1 MO would lead to more electron density localized on the metal. Experimentally, it is known that the tris(9,10-phenanthrenequinone)chromium complex with an overall charge of 2+ is EPR silent. According to Pierpont's formulation of these complexes a high-spin Cr(III) would be antiferromagnetically coupled to one SQ ligand and the 2+ complex should be paramagnetic by 2 electrons. Because of the delocalized nature of the MOs involved, simple ligand field arguments such as were used in the anionic series are not applicable. Further experiments, such as solution magnetic susceptibility measurements need to be performed in order to clarify the spin state of the 2+ complex. Oxidation of the 2+ complex yields the 3+ complex, whose molecular orbital diagram is shown in Figure 5a. Examination of the figure reveals the a_1–a_2 separation energy has increased. Not quite so obvious from the figure is the fact that the bonding is becoming less covalent (though not as dramatically as in the anionic series) with the 1e MO primarily metal in character and the 2e MO being primarily ligand in character. We have indicated the ground state of the 3+ complex to be a quartet on the basis of the simple crystal field calculations discussed earlier,[21] which yield a value for the spin-pairing energy over 3 times as large as the separation between the a_1 and 1e MOs. This quartet ground state would be in agreement with Pierpont's model for these complexes, which predicts a high-spin Cr(III) and three diamagnetic *o*-benzoquinone ligands, giving a complex with three unpaired electrons. The tris(9,10-phenanthrenequinone)chromium complex with overall charge of 3+ is also known to be EPR silent.[17] Further work needs to be done in order to clarify the spin state of the 3+ complex.

Table I. Charges on the Complex Fragments

	Mulliken charges[a]			
	Cr	BQ	SQ	CAT
$Cr(BQ)_3^{3+}$	1.73+	0.42+		
$Cr(BQ)_2(SQ)^{2+}$	1.79+	0.12+	0.03−	
$Cr(SQ)_2(BQ)^{+}$	1.88+	0.21−	0.33−	
$Cr(SQ)_3^{0+}$	1.95+		0.65−	
$Cr(SQ)_2(CAT)^{1-}$	1.86+		0.90−	1.06−
$Cr(CAT)_2(SQ)^{2-}$	1.74+		1.15−	1.29−
$Cr(CAT)_3^{3-}$	1.55+			1.52−

[a] Based upon a Mulliken population analysis. Charges for the ligands are relative to a neutral $O_2C_6H_4$ molecular fragment.

Considering the bonding in the entire series with the neutral complex as a reference point, we see as we move either to the right or to the left of the middle of Figure 5, reducing or oxidizing the neutral complex, that the bonding becomes more ionic and less covalent. Initially electrons are added to or taken from essentially nonbonding MOs (the a_1 on the metal or the a_2 on the ligands). Further reduction populates the 2e MOs, which are metal–ligand antibonding in character. On the other hand, continued oxidation results in the removal of bonding electrons from the 1e MO. Thus it is reasonable that there is a point beyond which the complexes cannot be further oxidized or reduced without decomposition. The cationic complexes are difficult to prepare and are substitution labile. We are unaware of any reports of a 4− tris(*o*-quinone)chromium complex, and we would predict, on the basis of our calculations, that such a species should not exist. As may be seen in Figure 5 the 3d orbitals are destabilized in gradually increasing amounts as we begin reducing the 3+ complex. Upon adding another electron to the 3− species, we would expect a further destabilization of the 3d orbitals resulting in occupied molecular orbitals above the zero in energy (even after accounting for the presence of counterions), which would be an unbound state and hence not stable.

As mentioned previously *o*-quinone ligands are "noninnocent", exhibiting a range of oxidation states. When transition-metal complexes of *o*-quinones are considered, the question of the metal and ligand oxidation states naturally arises. For example, is the neutral tris(*o*-quinone)chromium complex best formulated as a Cr(VI) and three catecholates or a Cr(III) and three semiquinones or a Cr(0) and three benzoquinones or possibly an intermediate chromium oxidation state with two different types of quinone ligands? If the assignment of formal oxidation states is an attempt to reflect the actual charge distribution in these complexes, then all of the above formulations are misleading.

To address the problem of the metal and ligand charge distribution, we present the results of a Mulliken population analysis[22] on our molecular orbitals for the seven-membered redox series in Table I. The charges given are relative to the

---

[22] Mulliken, R. S. *J. Chem. Phys.* **1955**, *23*, 1841–1846.

neutral atom or ligand. Thus, in free BQ the charge would be 0+, while in free SQ the charge would be 1− and free CAT would carry a 2− charge. The most striking feature about Table I is the trend in the charge on chromium over the seven-membered species. Over the span of a 6-unit change in the overall charge on the complex the charge on chromium changes by only 0.40 to an electron. Initially, though the overall charge on the comlex decreases as we go down the table, the charge on chromium increases slightly, reaching a maximum at the neutral species. Thereafter, the charge on chromium decreases, but by much less than the unit of charge that is added, despite the fact that the added electron occupies an MO that is localized on the metal. These small changes in the chromium charge and the trend in the charges for the cationic series may be explained by a consideration of the changes in bonding that take place as the complexes undergo reduction. There is a substantial rehybridization of the melt and ligand basis orbitals due to changes in their relative energies as a given complex is reduced. Because of this, regardless of whether the electron is added to a ligand- or metal-centered orbital, the charge is redistributed out onto the ligands.

Two points are worth noting about the charges on the ligands in Table I. First, it can be seen that the charges on the ligands usually deviate substantially from the free-ligand value. Second, in those cases where two different types of quinone ligand are present in the same complex (e.g., $Cr(BQ)_2(SQ)^{2+}$) a comparison reveals that the charge on BQ is always less negative than the charge on SQ and the charge on SQ is always less negative than that on CAT so that, even though the ligand charges deviate significantly from those of the free ligands, their relative magnitudes are what we would expect.

As mentioned earlier, the oxidation states of the ligands for tris(*o*-quinone) transition-metal complexes of the type considered here are usually assigned on the basis of crystal structures, the O–C, C1–C2, and M–O bond distances being quite characteristic. Crystal structures for complexes like the 1− or 2− complexes or the cationic complexes have not been reported. In order to be consistent with the experimental evidence, we had to perform our calculations using ligands of two different types for the 2+, 1+, 1−, and 2− complexes. Such structures are not without precedent, as the structures of a mixed-ligand cobalt complex, (3,5-di-*tert*-butylcatecholato)(3,5-di-*tert*-butylsemiquinone)(2,2′-bipyridyl)cobalt(III),[5] and a mixed-ligand molybdenum complex with two 9,10-phenanthrenequinone ligands of catecholate type and one of semiquinone type[23] have been published. Our calculations on the 1+ complex showed an energetic preference for the mixed-ligand type of complex. The data is Table I are consistent with a chromium whose charge remains essentially unchanged upon reducing the complex while the added charge is distributed roughly evenly over the ligands. For these reasons, we are in basic agreement with Pierpont's model for this seven-membered redox series of a chromium whose charge remains constant while successive additions of an electron reduce BQ ligands to SQ and then SQ ligands to CAT.

Summary

We have presented the results of Fenske–Hall approximate molecular-orbital calculations on a variety of different *o*-quinone transition-metal complexes. For the bis(*o*-quinone)(bipyridine)chromium 1+ complex the unpaired electron is predicted to occupy the metal-centered 2a MO, in accord with the observed large ^{53}Cr hyperfine coupling constant. On the basis of energy arguments, we predict the more stable structure for this complex is that in which the two *o*-quinone ligands are of the same type. Reducing this complex to form the bis(*o*-quinone)(bipyridine)chromium 1− complex causes an inversion of the 2a and 2b MOs resulting in the HOMO once again being the metal-centered 2a MO. The 1− complex is predicted to be low spin, which needs to be experimentally verified. In all cases, the HOMO–LUMO separation is extremely small and is outside of our previous experience with the Fenske–Hall method. Our results on the analogous tris(*o*-quinone)chromium 1− complex predict the HOMO to be the metal-centered a_1 MO, which also agrees with the EPR results. A 2-electron oxidation of the 1− complex to form the tris(*o*-quinone)chromium 1+ complex results in a dramatic decrease in the a_2–a_1 separation, but due to small errors in the off-diagonal elements of the approximate Fock matrix, there is no inversion of the a_2–a_1 order (which would most readily explain the observed large ^{53}Cr hyperfine coupling constant) as there was in the bis(*o*-quinone)(bipyridine)chromium calculations. Our calculations on the tris(*o*-quinone)vanadium neutral complex predict that the odd electron occupies the ligand-centered a_2 MO and are consistent with the small value of the ^{51}V hyperfine coupling constant for complexes of this type. The difference in the metal hyperfine coupling for vanadium and chromium has been rationalized on the basis of the greater stability of the 3d orbitals of chromium, which causes an inversion of the metal-centered and ligand-centered valence MOs when compared to the isoelectronic vanadium case.

Table II. Comparison of the 1-Electron Eigenvalues of the Frontier Molecular Orbitals

MO	$Cr(SQ)_3^{0+}$ ϵ_1[a]	$Cr(3,5\text{-}DMSQ)_3^{0+}$ ϵ_2	$\epsilon_2 - \epsilon_1$
1e	−10.78	−10.19	+0.59
a_2[b]	−9.56	−8.98	+0.58
a_1	−8.18	−7.60	+0.58
2e	−6.93	−6.34	+0.59

[a] Energies are in electronvolts. [b] Highest occupied molecular orbital.

Our results on the neutral and anionic members of the $[Cr(Q)_3]^n$ series predict there should be 0, 1, 2, and 3 unpaired electrons for the neutral 1−, 2−, and 3− complexes, respectively, in excellent agreement with the solution magnetic susceptibility measurements. Our calculations on these four complexes also reproduce the qualitative features of their visible absorption spectra—predicting a number of bands with large extinction coefficients for all except the 3− complex, which should exhibit a spectrum characteristic of d → d transitions only. For the cationic series of tris(*o*-quinone)chromium complexes we predict the ground state of the 2+ complex should be a singlet and the ground state of the 3+ complex should be a quartet, although there are no confirmatory experimental data on these complexes. The results of our calculations on the entire seven-membered series show that, as one gets further away from the neutral complex in charge, the metal–ligand bonding becomes weaker. We predict that 4− species should not exist because of the trend in the destabilization of the chromium 3d orbitals. A consideration of the metal and ligand charges over the seven-membered series leads us to agree with Pierpont's formulation of this series as a chromium whose charge remains essentially constant while the electrons are added to the ligands. We predict that there are two different types of $O_2C_6H_4$ ligands bound to the chromium in the 2+, 1+, 1−, and 2− complexes; this has yet to be verified crystallographically. The differing properties of the members of the series are most easily explained as a result of the effects on metal–ligand bonding brought about by the dramatic change in the stability of the 3d orbitals as the complexes are reduced.

---

(23) Pierpont, C. G.; Buchanan, R. M. *J. Am. Chem. Soc.* **1975**, *97*, 4912–4917.

Acknowledgment. We thank Professor C. G. Pierpont for many useful discussions and communication of his results prior to publication. This research was supported by National Science Foundation Grant CHE78-24882.

Appendix

When we first attempted to compare the results of our calculations on the transition-metal quinone complexes with experimental results, a difficulty arose. The experimental data exist primarily for the 3,5-di-*tert*-butyl-1,2-benzoquinone (3,5-DBQ); 3,4,5,6-tetrachloro-1,2-benzoquinone (*o*-Cl_4Q), and 9,10-phenanthrenequinone (9,10-phenQ) ligands, with very few data on the unsubstituted *o*-benzoquinone ligand. Because of the large number of atoms (and hence basis functions) involved, it is not possible for us to do a complete tris(*o*-quinone)chromium complex calculation with our present facilities for the 3,5-DBQ or 9,10-phenQ ligands, while calculations using the *o*-Cl_4Q ligand are very time consuming. We hoped that the majority of the features of our calculations on the unsubstituted *o*-quinone complexes would carry over to the larger systems so that they could be used to model the systems we are unable to perform calculations on.

In order to see what effect changing the *o*-quinone ligand would have on our calculations, we undertook a series of tris(*o*-quinone)chromium calculations using 3,5-dimethyl-1,2-benzoquinone (3,5-DMQ) and *o*-Cl_4Q as ligands. For the 3,5-DMQ ligand overall charges of 1+, 0, 1−, and 3− were considered, while for the *o*-Cl_4Q ligand the neutral and 1− complexes were used. In all cases examined, the character of the frontier orbitals remained essentially unchanged. The main effect of changing the quinone ligand was to shift the energy levels to more positive values. A comparison of the eigenvalues of the frontier orbitals of the neutral tris(*o*-quinone)chromium complexes with SQ and 3,5-DMSQ as quinone ligands is presented in Table II along with the difference between corresponding eigenvalues. An examination of the table reveals the shift to more positive energies is essentially constant and is not dependent on whether the MO is occupied. This is true of all the 3,5-DMQ calculations we peformed. For the *o*-Cl_4Q ligand there are two shifts, one for occupied levels and another for unoccupied MOs. However, in all cases considered the order of the MOs remained unchanged. (We were unable to get a 1+ complex calculation using the *o*-Cl_4Q ligand to converge due to oscillatory crossing of the a_2 and a_1 MOs because they are so close in energy. Recall, however, an inversion of their order relative to the $Cr(SQ)_2(BQ)^+$ calculation would more readily agree with the experimental evidence.)

It is interesting to note that the difference in energy between the $3b_1$ orbitals for free-ligand calculations on SQ and 3,5-DMSQ is −0.41 eV. The free-ligand calculation on 3,5-DBSQ is very similar to that of 3,5-DMSQ. Because of the similarity in the methyl- and *tert*-butyl-substituted-free-ligand calculations and the small changes in the tris(*o*-quinone)chromium complex calculations upon changing from the unsubstituted quinone ligand to the 3,5-DMQ ligand, we feel confident our results on the unsubstituted quinone complexes would carry over to 3,5-DBQ complexes. We have also performed free-ligand calculations on 9,10-phenQ. The main difference between these calculations and those on the unsubstituted quinone is a (larger than for 3,5-dialkyl group substitution) shift of the $3b_1$-like orbital to more positive energy. The $3b_1$-like orbital should have the most influence on the frontier orbitals because it is the ligand orbital that contributes most significantly to them. Given the similarity of the EPR data on the *o*-Cl_4Q, 9,10-phenQ, and 3,5-DBQ complexes and the similar behavior of our free-ligand calculations on the 3,5-DMQ, 3,5-DBQ, 9,10-phenQ, and *o*-Cl_4Q ligands, we believe we are justified in making comparisons of the results of our calculations on the unsubstituted tris(*o*-quinone)chromium complexes with experimental data on the larger ligand systems for which we cannot perform calculations on the entire complex.

Registry No. $Cr(BQ)_3^{3+}$, 81876-03-1; $Cr(BQ)_2(SQ)^{2+}$, 81876-04-2; $Cr(SQ)_2(BQ)^+$, 81876-05-3; $Cr(SQ)_3^{0+}$, 81857-51-4; $Cr(SQ)_2(CAT)^-$, 81875-97-0; $Cr(CAT)_2(SQ)^{2-}$, 81875-98-1; $Cr(CAT)_3^{3-}$, 81875-99-2; $Cr(bpy)(SQ)_2^+$, 81876-00-8; $Cr(bpy)(SQ)(CAT)^{0+}$, 81876-01-9; $Cr(bpy)(CAT)_2^-$, 81876-02-0; $V(SQ)_3^{0+}$, 81857-52-5.